Proceedings World Geothermal Congress 2010
Bali, Indonesia, 25-29 April 2010

3-D Numerical Models for Temperature Prediction and Reservoir Simulation

Darius Mottaghy, Renate Pechnig, Nick Buik, Erik Simmelink

Lütticherstr. 32, D-52064 Aachen, Germany

d.mottaghy@geophysica.de

Keywords: Geothermal reservoir, numerical modeling, thermal conductivity

ABSTRACT

The prediction of reservoir temperatures and production behavior is crucial for planning a deep geothermal installation. We present a study regarding these issues using the example of a planned doublet in a Jurassic sandstone layer in the city of The Hague, The Netherlands.

In the first phase, the main objective is to find out whether there is a significant influence of the 3-dimensional structures of anticlines and synclines on the temperature field. To achieve this target, comprehensive petrophysical investigations were performed and a large scale 3-D-model has been built up. Several bottom hole temperatures, as well as petrophysical logs available in the area were used to calibrate the model. Profiles and cross sections extracted from the calculated temperature field allow a detailed study of the temperature in the surrounding of the planned location. Test runs with different thermal conductivities for each layer showed the importance of a proper determination of this thermal parameter for a reliable temperature prediction.

In the second phase of the project, a detailed 3-D numerical reservoir model was set up. The temperature model from the first phase provided the boundary conditions for the reservoir model.

Hydraulic parameters for the target horizons such as porosity and permeability were taken from data available from the nearby exploration wells. The aim is to predict the temperature evolution, both at the producer and injector location. The main interest lies in the issue whether production temperatures can be maintained throughout the years or not, and how far the cooling area around the injector extends. Several runs were performed, varying the hydraulic properties in a reasonable range. The geometry was modified as well, according to different locations of the producer. The model was designed in order to ensure its long term usage in the project. To accomplish this, the model will be constructed to allow iterative updates, assimilating new information gained during the drilling, testing and production phase.

1. INTRODUCTION

In the frame of the "Den Haag Zuidwest" district heating system, a deep geothermal installation is projected. It is intended to provide heating for 6000 houses with a geothermal power of about 5 MWth. The target horizon of the planned doublet is the "Delft sandstone", an upper Jurassic sandstone layer, which has been extensively explored for oil and gas reservoirs in the last century. In the target area, this layer is found at a depth of about 2200 m with an average thickness of 50 m. An additional target layer is the overlying "Rijkswijk Sandstone", with an additional thickness of about 25 m. The thicknesses were estimated for the target area from existing oil and gas exploration wells located in the neighborhood. Since these layers cannot be resolved by seismic interpretation, a direct mapping is not possible at the current stage of the project (Simmelink and Vandeweijer, 2008).

Within the project, several studies have been performed in order to provide information on temperature and production rates for the geothermal installation wells. Temperature predictions were made extrapolating the temperature data from the neighboring oil and gas exploration wells (see Figure 1). Hydrocarbons were explored and produced only from the NNW-SSE striking anticline structures. In contrast, the doublet is planned to be drilled into a syncline in order to achieve higher production temperatures from the water filled sand-stone formation. The synclines have not been drilled in hydrocarbon exploration, thus no direct information on temperature are available. This is also valid for the hydraulic properties, which are only known from the exploration wells.

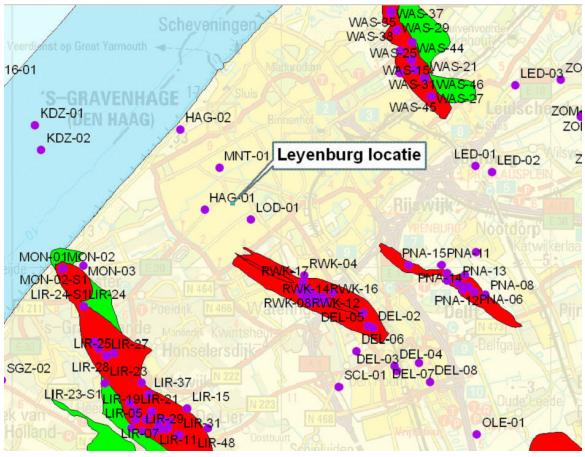

Figure 1: Location (Leyenburg) of the geothermal installation and the existing exploration wells. The production well will be deviated to the NE to reach the syncline structures.

Thus, this project aims to predict the temperature field and study the influence of the subsurface heterogeneity in the first phase. After that, a reservoir model based on the regional model is built in order to characterize the performance of the running doublet.

2. REGIONAL TEMPERATURE MODEL

The procedure for building a 3-D regional temperature model was based on the following four working stages.

2.1 Acquisition and Compilation of Basic Data Sets

The construction of the model requires information of the whole strata overlying and, as far as available, underlying the Upper Jurassic target reservoir. Thus, the first step was to collect information on the subsurface geometry, depth and

thickness of the stratigraphic layers. The basic geological model was provided by TNO. Information on the formation's petrophysical properties were derived from log and laboratory data. At this stage, quality and amount of log data and the availability of core and cutting materials were checked for the exploration wells in the surrounding of the target area. Table 1 summarizes this data. Two key wells were selected which provided representative information on the subsurface. Log data and cuttings data from these wells were used for the further analyses.

2.2 Laboratory Measurements on Cuttings Samples

To gain direct information on the thermal properties of the subsurface, rock samples were taken from the drilling material of the key wells. Samples were taken more or less equally spaced from Upper Carbonifereous to Upper Cretaceous stratigraphic layers. A total of about 80 samples were collected from the storage. From these samples 50 were finally measured in the laboratory. Thermal conductivity measurements were performed by a line source equipment (TK04).

The thermal conductivity values exhibit considerable variations for the matrix of the rock samples. The distribution is shown in the histogram of Figure 2. Two groups can be divided: The rocks with matrix conductivities λ_m <3.0 W m^{-1} K^{-1} are mainly claystones and carbonates e.g. from the Altena and the cretaceous rock series. Rocks with higher values of λ_m m >3.0 W W m^{-1} K^{-1} were measured in the sandstone rich units of the Jurassic/Cretaceous transition sequence and the Triassic Bunter series. The grain density values show a normal distribution (Figure 3) with a mean value of 2.68 g cm^{-3}.

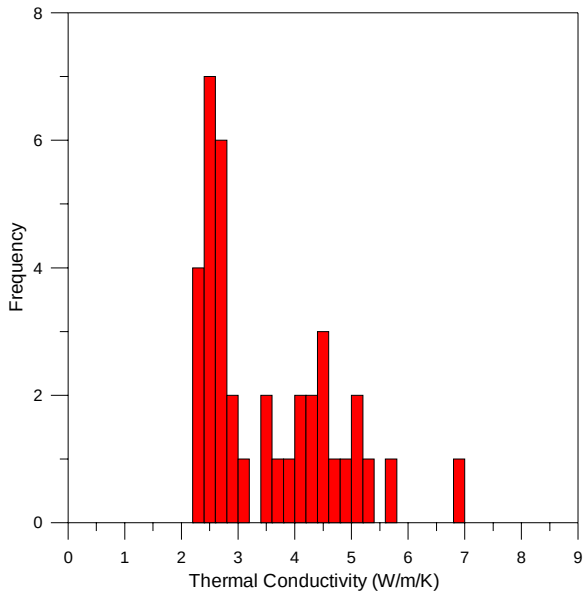

Figure 2: Histogram of the measured thermal conductivity of the rock matrix.

Table 1: Listing of the wells and availability of core and log data in the surrounding of Den Haag. LOGS: SP= Self Potential, res= Resistivity, gr= Gamma-Ray, dt= Sonic Traveltime, rhob= Bulk density, nphi= Neutron Porosity; CORE: KNNSR= Rijswijk Member, SLDND= Delft Sandstone.

Available log- en coredata

Boring	Yr	Analogue		Digital					Coredata
		SP	res	gr	dt	rhob	nphi	Res	
BRK-03	1955								
DEL-08	1994			gr	dt	rhob	nphi	Res	
HAG-01	1954	SP	Res						KNNSR
HAG-02	1955	SP	Res						KNNSR
KDZ-02	1986			gr	dt	rhob	nphi	Res	
LED-01	1956								KNNSR
LIR-45	1982			gr	dt	rhob	nphi	Res	KNNSR
MED-01	1958								KNNSR
MON-01	1956								KNNSR
MON-02	1982			gr	dt	rhob	nphi	Res	KNNSR
MON-03	1990			gr	dt	rhob	nphi	Res	
PNA-02	1955								KNNSR, SLDND
PNA-03	1955								KNNSR
PNA-04-S2	1981			gr		rhob	nphi		
PNA-07	1957								KNNSR
PNA-10	1957								KNNSR
PNA-14	1985			gr	dt	rhob	nphi		
PNA-15	1994			gr		rhob	nphi		
RTD-01	1984								SLDND
RWK-01	1953								KNNSR, SLDND
RWK-02	1953								KNNSR
RWK-03	1953								KNNSR
RWK-04	1954								KNNSR
RWK-05	1954								KNNSR
RWK-06	1954								KNNSR
RWK-07	1954								KNNSR
RWK-08	1955								KNNSR
RWK-09	1955								KNNSR
RWK-11	1956								KNNSR
RWK-14	1956								KNNSR
RWK-18	1954			gr	dt				
Q13-07-S2	1990			gr	dt	rhob	nphi	Res	
Q14-01	1984								KNNSR
Q16-01	1970			gr	dt			Res	KNNSR
Q16-02	1978			gr	dt	rhob	nphi	Res	
WAS-01	1956								KNNSR
WAS-02	1957								KNNSR
WAS-05	1957								KNNSR
WAS-23	1960			gr	dt	rhob	nphi	Res	KNNSR

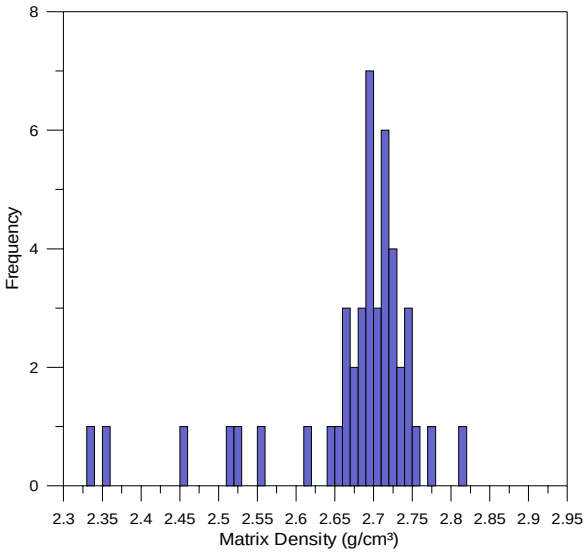

Figure 3: Histogram of the measured grain density of the cuttings samples.

2.3 Determination of Thermophysical Properties for the Stratigraphic Units Based on Laboratory and Log Data

During this stage an integrated analysis of laboratory measurement with log data was performed in order to provide thermal property input parameter for layers of the 3-D model. Readings of wireline logs respond to the composition of the probed rock, its structure and environmental conditions. For the analysis of borehole geophysical data in terms of the quantitative description of the rock composition, the assumption was made that a log reading responds mainly to the composition of the rock, given some appropriate mixing laws. Using a standard procedure, the shale content and the free water content were computed for the key wells. In turn these data were used to compute thermal conductivity profiles (Hartmann et al., 2005; 2007). The log derived thermal conductivity profiles were calibrated with the laboratory measurements. This is shown in Figure 4 for one of the key well. Here, the right column shows the good agreement between measured and interpreted data. Using these profiles, statistical values of effective thermal conductivity were calculated for the stratigraphic units incorporated in the 3-D model. In addition, radiogenic heat production profiles were produced by the use of the gamma-ray logs (Bücker and Rybach, 1996). The log derived profiles served two purposes. First, the variability of the downhole thermal conductivity could be better assessed based on continuous wireline data compared to discrete cuttings data, which might be subject of preferential sampling. Second, the number of boreholes allowed a better spatial characterization of facies changes and the corresponding changes of petrophysical properties.

2.4 Built up and Test of a 3-D Numerical Model and Simulation Runs

In this last working stage the regional 3-D model was set up, using the data and information gathered in steps 1 to 3.

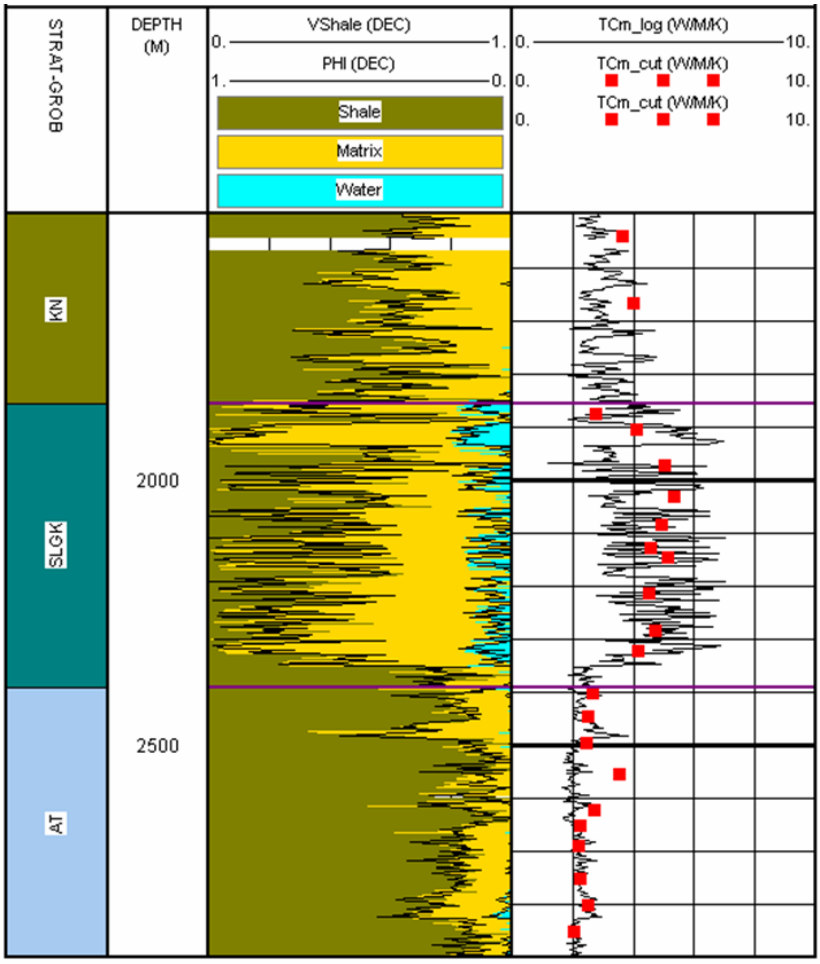

Figure 4: Calculated thermal conductivity of the rock matrix compared with the laboratory measurements, shown exemplary for the depth level 1500-2900 m.

2.4.1 Numerical Tool

The 3-D finite difference (FD) code SHEMAT (Simulator for Heat and Mass Transport, Clauser, 2003) is used for the 3-D numerical simulation of heat flow in the Den Haag area. SHEMAT solves coupled problems involving fluid flow, heat transfer, species transport, and chemical water-rock interaction in fluid saturated porous media. For the temperature model, a purely conductive regime is presumed. The flat topography around Den Haag is not able to trigger any significant flow which may affect the subsurface temperature. Deeper flow fields with a major influence due to advective heat transfer are not known so far.

The aim lies at establishing the baseline of the temperature distribution in the area of the planned geothermal installation at a larger scale. Steady-state simulations yield an estimate of the order of magnitude of the temperature distribution, in particular in the target horizon. This steady state temperature field is affected by the spatial distribution of thermal conductivity and other parameters, as well as the boundary conditions such as surface temperature and heat flow.

2.4.2 Model Setup

The three dimensional rectangular grid for the FD simulations covers the regional area around Den Haag as shown on the map in Figure 5. The planned drilling location is marked by a pink circle. The model extends over 22.5 km×24.3 km with 5 km depth, and thus, the lower boundary lies within the carboniferous basement. The numerical grid consists of 2,430,000 nodes, horizontally and equally spaced by 150 m and vertically by 50 m. For creating the grid the software Argus One (TM) was used. The model's general properties are listed in Table 5-4. On the ground surface a constant mean annual temperature of 11°C is assumed which is slightly above the mean annual air temperature of 10°C at 2 m height in the area. The fact that mean ground surface temperatures are slightly above mean air surface temperatures is generally observed and there have already been several studies (e.g. Smerdon et al., 2006). The lower boundary condition is represented by the basal heat flow. It is only vaguely determined in the area (60-70 mW m^{-2}, Hurter and Haenel, 2002), thus it is a parameter to be adjusted by comparison with available in-situ temperature data (see next section).

Table 2: Properties of the 3-D model.

Parameter	Value
Mesh Size;Resolution	150 × 162 × 100; 150 m × 150 m × 50 m
Number of nodes	2,430,300
Basal heat flow q	63 mW m^{-2}
Surface temperature	11°C
Geological Units	9
Thermal boundary condition	On the surface: const. T, bottom: constant q
Thermal conductivity	f(T)

The model comprises nine units, of which TNO (Simmelink et al., 2007) delivered the necessary information on depths which were obtained by seismic survey. Table 3 summarizes the units' properties in terms of thermal conductivity and heat production, determined on rock samples and logging data (see section 2.3). For the North Sea Group as well as the basement, no drilling material was available, therefore this additional data has to be taken from the literature (Norden and Förster, 2006). Figure 6 shows the 3-D model with the geological units and the temperature distribution.

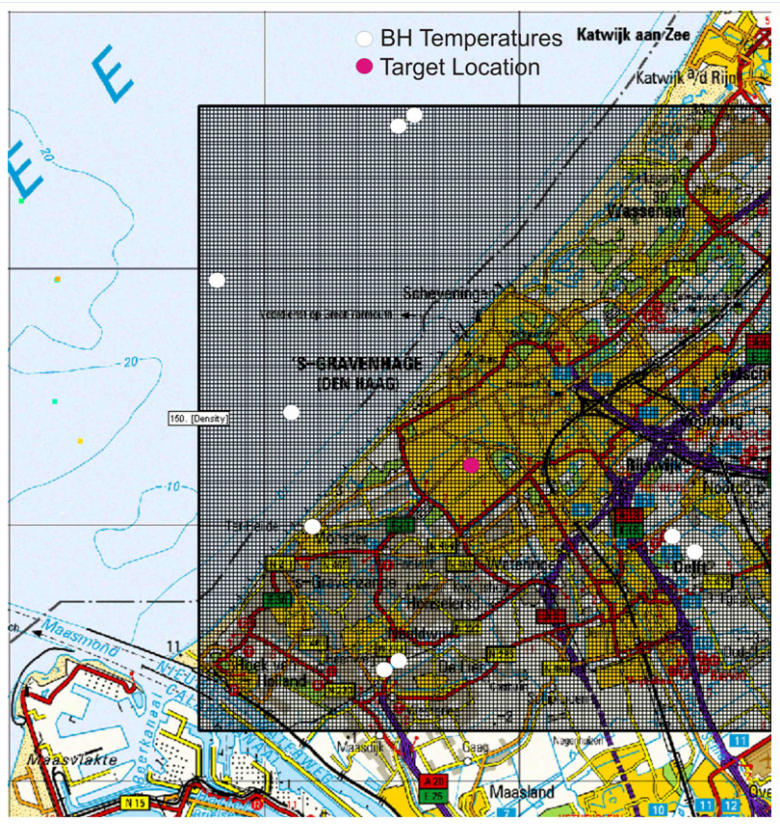

Figure 5: Location of the FD grid, together with the target location and BHT data available.

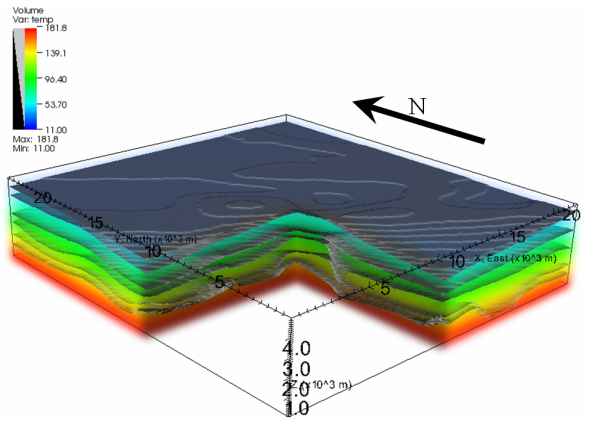

Figure 6: Sketch of 3-D model, showing the geological layers and the temperature distribution in °C.

Table 3: The nine lithological units and their thermal parameters. Values are restricted to the investigated area.

Unit	Bulk thermal conductivity, ± standard deviation (W m^{-1} K^{-1})	Heat generation rate (mW m^{-3})
North Sea Supergroup (N)	2.3	1.05
Upper Cretaceous Supergroup (CK)	1.80– 2.20 – 2.60	0.46
Lower Cretaceous Supergroup (KN)	1.94 – 2.51 – 3.08	0.92
Jurassic Supergroup (S)	2.93 - 3.75 – 4.57	0.75
Altena (AT)	1.81 – 2.17 – 2.53	1.44
Lower Germanic Trias Group (RB)	1.93 – 2.80 – 3.67	1.61
Zechstein (ZE)	1.93 – 3.14 – 4.35	1.33
Rotliegend (RO)	4	0.75
Basement (DC)	2.3	2.30

Model calibration

Several corrected bottom hole temperatures (BHT) in the study area were made available by TNO. All these BHT are also corrected for true vertical depths. The small number of data points only allows a very limited calibration of the model regarding the basal heat flow. However, several model runs yielded a good estimation for the basal heat flow of 63 mW m^{-2}.

Figure 7 shows the comparison of the temperature profile at the target location taken from the model. The stratigraphy is plotted as well, with color codes according to those used in Simmelink et al. (2007). This figure shows (dashed lines) the strong sensitivity to thermal conductivity. The values are varied within the standard deviation (Table 3). Here, the importance of a proper determination of thermal conductivity becomes evident. The deviation from the mean value of the temperatures when using the lower and the higher limits of thermal conductivity becomes as large as 10 K at reservoir depth of about 2 km.

Results

In order to predict reliable temperature distributions around the planned drilling site, the resulting temperature distribution within the model using the mean values in Table 3 is studied more closely. The target reservoir, the Delft sandstone, lies just beneath the KN surface, so temperatures at this depth are plotted in Figure 8. From this figure, the optimal drill trajectory in terms of temperature can be estimated. The highest temperatures of 79-80°C are found directed NNE from the target location, in the synclinal structure of the KN layer.

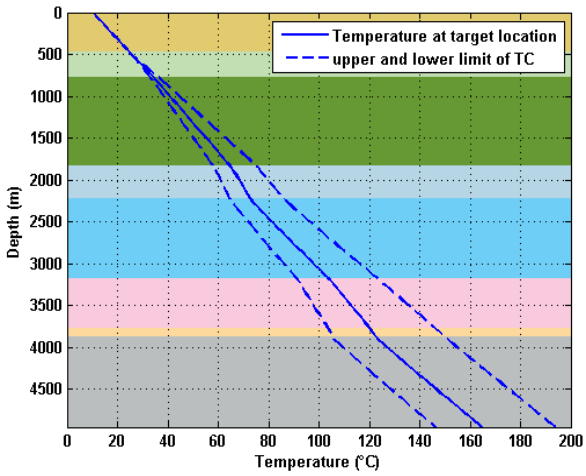

Figure 7: The temperature profile extracted from the model at the target location. The dashed lines show the upper and lower limit resulting from varying thermal conductivity (TC) within the standard deviation (see Table 3).

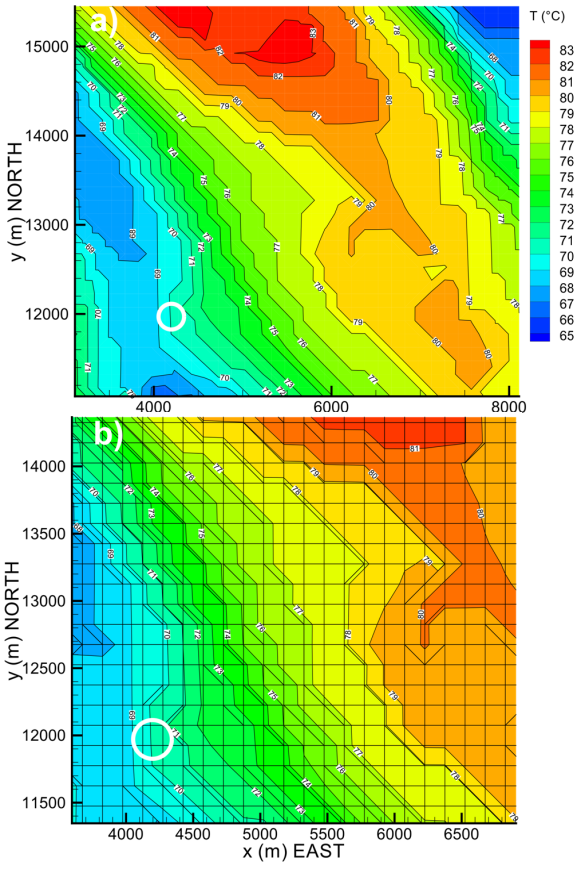

Figure 8: Temperature distribution along the KN Base at different scales. The white circle indicates the planned drilling location at Leyenburg.

In Figure 9, a horizontal section at 2300 m depth is plotted which clarifies the importance of a 3-D study: at the same depth the lateral temperature variation can reach almost 10 K difference, due to the subsurface geometry and the different thermal properties of the geological units.

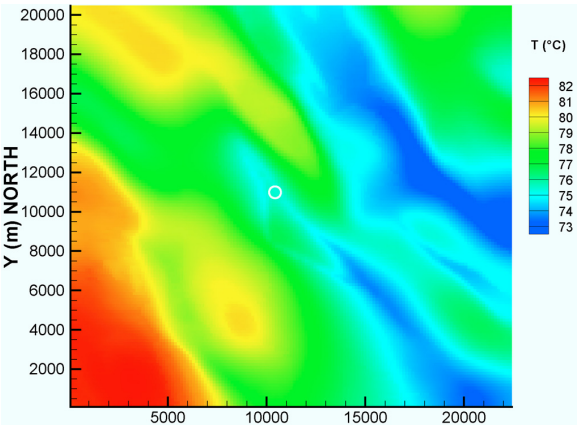

Figure 9: Temperature distribution at a constant depth of 2300 m for the whole model. The white circle indicates the planned drilling location.

3. 3-D RESERVOIR MODEL

In the second phase of the project, a detailed reservoir model was set up. The aim is to predict the temperature evolution both at the producer and injector locations. The main interest lies in the issue if production temperatures can be maintained throughout the years, and how far the cooling area around the injector extents.

3.1 Model Setup

The model itself is based just like the regional model on seismic interpretations by TNO (Simmelink et al., 2007, Simmelink and Vandeweijer, 2008), with the newer one for the KN Base. In addition to the thermal parameters, hydraulic properties enter the simulations now. The crucial parameter permeability was re-evaluated by Simmelink and Vandeweijer (2008) for the reservoir, the Delft sandstone. It extends over a range from 250 mD to 2 Darcy, with a mean of 500 mD. Different transmissivities arise from different reservoir thicknesses and permeabilities. Since it is more convenient to keep the reservoir geometry constant when performing sensitivity studies, the mean value determined by TNO (2008) for the Delft sandstone is kept at 55 m. Only permeabilities were varied. This in turn yields different transmissivities, as shown in Table 4.

The general properties of the reservoir model are shown in Table 5. Due to the high computing demand of this transient model, which must be run for several tens of years, it must be kept as small as possible. However, it must account for all details and be numerically stable, nevertheless, which in turn requires a certain number of grid cells. This model is thus a result of several model-setups and test runs, representing an optimum. At the locations of the injector and producer, the grid is refined in order to deal with the higher fluid velocities at these points. Figure 10 shows an overview of the model where this refinement is visible. The locations of the producer and injector are indicated as well. During the course of the project the planned producer location was modified, taking the model results into account. The location shown here represent the latest set up, referring to the final depths of the deviated boreholes (about 1800 m for the injector and 2230 m for the producer) and not to the actual drilling location on the surface. Figure 11 shows the integration of the reservoir model with the large scale temperature model. Boundary conditions and parameters of the reservoir model were adapted to fit with the results of the temperature model.

Table 4: Permeability and transmissivity of the Delft sandstone. In the model, the thickness of the reservoir is kept constant at the mean value of 55 m, a variation of permeability in the different model runs corresponds to the shown transmissivity values.

Permeability	Transmissivity
100 mD	$5.5*10^{-5}$ m^2 s^{-1}
500 mD	$2.75*10^{-4}$ m^2 s^{-1}
1000 mD	$5.5*10^{-4}$ m^2 s^{-1}

Table 5: Properties of the 3-D model.

Parameter	Value
Mesh Size, Resolution	64 × 41 × 65; 25-100 m × 25-100 m × 17 m
Number of nodes	170 560
Extension	5.5 km x 3.5 km
Top	1500 m
Bottom	2605 m
Temperature at top	55.8
Basal heat flow q	67.8 mW m^{-2}
Top Delft	75 m below bottom KN
Bottom Delft	130 m below bottom KN
Thermal boundary condition	On the surface: const. T, bottom: constant q
Porosity	15 %
Permeability	100 mD – 1000 mD
Injection and production rate	150 m^3 h^{-1}
Temperature of injected water	40 °C
TC matrix Delft	5.6 W m^{-1} K^{-1}
Thermal conductivity	f(T)

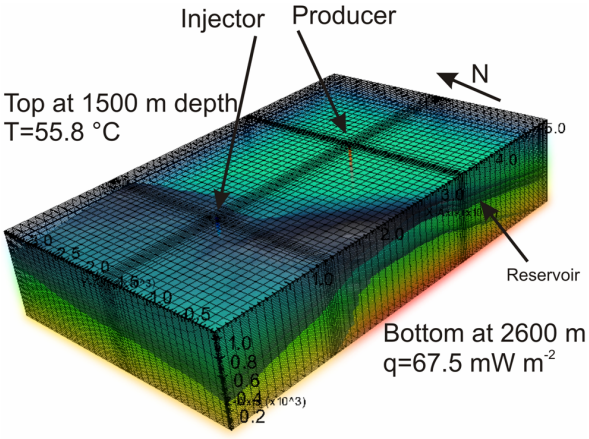

Figure 10: Sketch of the reservoir model, showing the grid and the layers, as well as the position of the producer and injector. The grid is refined at these locations. The y-axis is rotated by 8 degrees from north counterclockwise.

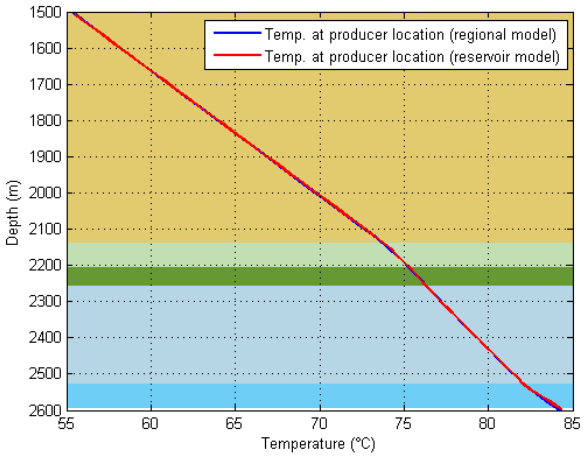

Figure 11: Vertical temperature profile at the (alternative) producer location. The parameters of the reservoir model are adapted to match the result from the larger, regional model. The Delft sandstone is represented by the green layer.

3.2 Results and Discussion

The transient simulations require a steady-state temperature and flow field as an input. An individual steady-state simulation had to be performed, one for each different permeability (Table 3).

By performing these steady-state simulations, it turned out that in the case of the lowest permeability, the maximum Darcy-velocity is less than 4 mm per year. When assuming 500 mD for the reservoir, it rises to 3 cm per year, and for 1000 mD it becomes 20 cm per year at maximum. The latter high permeability value is rather unlikely to be uniformly distributed, and the mean flow velocities are much lower. Furthermore, the flow field does not show large areas of preferential flow directions. Therefore it can be concluded that the steady-state situation is dominated by conductive heat transport. This in turn justifies a posteriori the assumption of purely conductive heat transport in the regional model.

After the steady-state simulations, the transient modelling was initiated, simulating the running system with producing and injecting water. The simulation was run over 50 years with varying time step length from a few hours at the beginning to one day later. This procedure accounts for the higher gradients of thermal and hydraulic parameters of the injection process when starting the simulation. These gradients gradually decrease later. The simulations were run on an Opteron Workstation, taking advantage of parallel computing on all 4 CPUs available. The total computing time ranged from 4-8 days, depending on the hydraulic parameters.

Figure 12 shows the temperature development at the producer's location at 2230 m depth. The different colors indicate the different permeabilities set. In each case there is only a small temperature drop of approximately 1.5 K over 50 years.

The corresponding temperature field shows a significant cooling within a radius of less than 1 km around the injector. Longer test runs show that a first “thermal breakthrough” does not occur until 90 years after starting the injection. Furthermore, the fluid coming from the injector is almost in equilibrium of the surrounding at the producer after this time. Therefore, even within this time scale, no significant temperature drop can be expected.

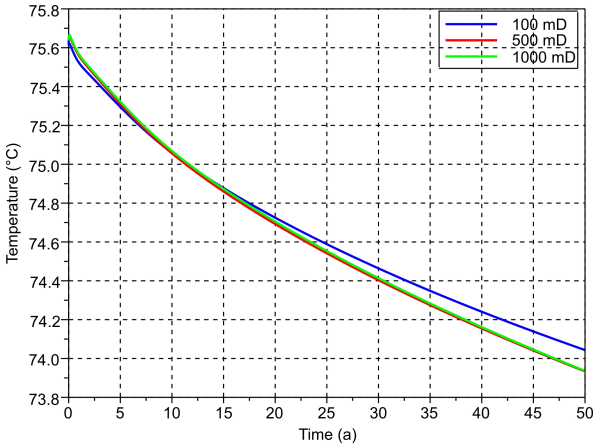

Figure 12: Temperature development at the depth of the alternative producer location (~2230 m) within 100 years, for different permeabilities of the reservoir.

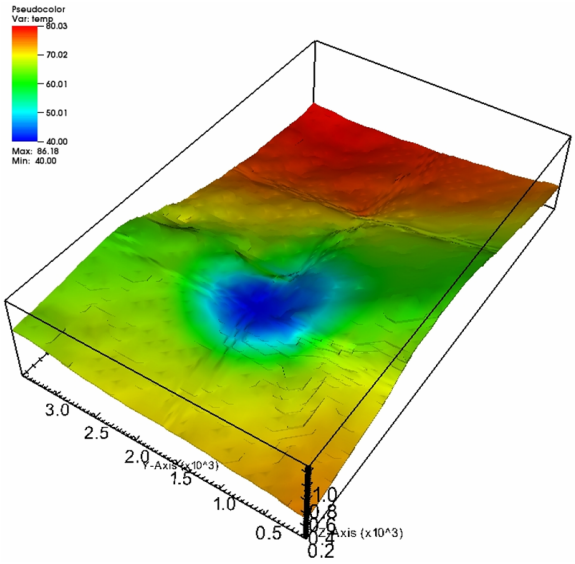

Figure 13: Temperature in °C at the top of the Delft sandstone after 100 years of injection (permeability is 500 mD), using the modified model with the producer being closer to the injector.

4. CONCLUSIONS

The results of the temperature model show that the use of large scale 3-D simulation is crucial for planning a deep geothermal installation. Due to the heterogeneity of the subsurface, regarding basin geometry and thermal properties temperatures may deviate from a simple geothermal gradient. For example, here a variation of 10 K is observed in a depth level of 2300m, which is the approximately reservoir depth at the producer location.

The reservoir models show encouraging results since no significant thermal breakthrough can be expected. In the first case with the originally planned location of the producer, the extracted water is predicted to be around 79 °C, with an almost negligible cooling in the first 50 years of production. In the model presented here, where the producer is closer to the drilling location, the shallower depths of the reservoir

yield lower water temperatures of around 75 °C. There is also a larger decrease in temperature with time. After 100 years a drop by 2.5 K can be expected. This is due to the fact that the reservoir is steeper here, thus cooler water can more easily move downwards.

For all these results, there are a number of constraints to be regarded. First of all, the calibration of these models depends on rather sparse temperature data which makes it hard to come up with some absolute uncertainty in temperature values. However, the laboratory measurements together with log interpretation are a very good basis to complement the poor data basis.

Any mechanical clogging of the borehole during the pumping process is not considered in the model. Other approximations are the isotropic and homogenous permeability, as well as the neglect of any stress field and faults. Furthermore, data is sparse on permeability itself and only known from existing synclinal borehole data.

Regarding all these latter issues about the uncertainty of thermal and hydraulic parameters, there is an ongoing study in cooperation with the Aachen University. Certain geological units of the 3-D models will be modified in terms of statistical variation of thermophysical parameters. Several model runs will then yield a parameter estimation which will give in turn hints on the uncertainty in temperature prediction. This study is presented in an accompanying paper entitled “Quantifying uncertainty in geothermal reservoir modeling”.

ACKNOWLEDGEMENTS

We thank IF Technology (Arnheim, Netherlands) and TNO Built Environment and Geosciences (Delft, Netherlands) for providing data and granting permission to publish results, as well as Eneco Energy (Rotterdam, Netherlands) and E.ON Benelux (Rotterdam, Netherlands) for initiating and funding the districted heating project in The Hague, from which these data are derived.

REFERENCES

Bücker, C. and Rybach, L.: A simple method to determine heat production from gamma-ray logs, Marine and Petroleum Geology, 13, 373-377, (1996)

Clauser, C. (ed.): Numerical simulation of reactive flow in hot aquifers using SHEMAT and Processing Shemat. Springer Verlag, Heidelberg-Berlin, (2003)

Hartmann, A.; Rath, V. and Clauser, C.: Thermal conductivity from core and well log data, International Journal of Rock Mechanics & Mining Sciences 42, 1042-1055, (2005)

Hartmann, A., Pechnig, R., and Clauser, C.: Petrophysical analysis of regional-scale thermal properties for improved simulations of geothermal installations and basin-scale heat and fluid flow. International Journal of Earth Sciences, (2007), DOI 10.1007/s00531-007-0283-y

Hurter, S. and Haenel, R. (eds.): Atlas of Geothermal Resources in Europe. Lovell Johns Ltd, (2002)

Norden, B. and Förster, A.: Thermal conductivity and radiogenic heat production of sedimentary and magmatic rocks in the Northeast German Basin, AAPG Bulletin, 90, 6, 939-962, (2006)

Simmelink, H.J.; Vandeweijer, V.; and Ramaekers, J.: Geologisch locatie-specifiek onderzoek voor het Buisiness Plan Geothermie Den Haag Zuid-West. TNO-rapport 2007-U-R1118/B, Utrecht, (2007)

Simmelink, H. J. and Vandeweijer, V.: Geothermie Den Haag Zuid-West, 2e fase geologisch onderzoek. TNO-rapport, Utrecht, (2008)

Smerdon, J.E.; Pollack, H.N; Čermák, V.; Enz, J.W.; Krešl, M.; Šafanda, J.; and Wehmiller, J.F.: Daily, seasonal, and annual relationships between air and subsurface temperatures. Journal of Geophysical Research. 111, D7, (2006)